

A Wireless Biomimetic Underwater Microrobot for a Father-son Robot System

Maoxun Li¹, Shuxiang Guo^{2,3}

¹ Graduate school of Engineering, Kagawa University, 2217-20, Hayashichou, Kagawa, Japan

² Key Laboratory of Convergence Medical Engineering, System and Healthcare Technology, The Ministry of Industry and Information Technology, School of Life Science, Beijing Institute of Technology, No. 5, Zhongguancun South Street, Haidian District, Beijing 100081, China

³ Department of Intelligent Mechanical Systems Engineering, Kagawa University, Takamatsu, Kagawa 761-0396, Japan
s14d505@stmail.eng.kagawa-u.ac.jp, guo@eng.kagawa-u.ac.jp

Abstract – A father-son underwater robot system is proposed for the underwater intervention in our previous research. In this system, the underwater microrobots used as the mechanical arms are carried by a high-speed amphibious spherical father robot and controlled by the robot with cables. In this paper, a smart actuator-based wireless microrobot is designed and developed as the mechanical arm of the father robot to recycle the small object. The biomimetic son robot is actuated by nine ICPF (ionic conducting polymer film) actuators, which can realize the basic motions including walking, rotating and grasping motions. To implement the communication between the father robot and the wireless microrobots, a new cableless communication method is proposed. The father robot uses two LEDs (light-emitting diodes) to send signals to control the motion of microrobots and used a Wi-Fi camera module to catch the feedback signals from the microrobots. Two light sensors and two indicator lights are equipped on the microrobot. Moreover, the father robot can send out and receive the microrobot with the fixture mechanism and the LED tracking mechanism. We evaluated the performance of the basic motions of the microrobot. Finally, we carried out the experiments to verify the communication protocol.

Index Terms – Underwater microrobot, Father-son robot configuration, Manipulator, Communication protocol, Tracking motion.

I. INTRODUCTION

With the growing importance of underwater intervention, underwater vehicles including AUVs (autonomous underwater vehicles) and ROVs (remotely operated vehicles) have been applied to intervention tasks progressively. To perform an underwater mission, the underwater manipulators are the crucial equipment of the underwater vehicles. Typically, ROVs are operated by human to perform the underwater manipulation [1]. However, ROVs are generally equipped with the bulky multi-link arms and requires a mother ship to dock, which restricts their positioning and performance of manipulation.

In contrast, AUVs can achieve a better performance of positioning and flexibility than ROVs, because they do not require the mother ship and the tether. Recently, AUVs equipped with the underwater manipulators are few. A reconfigurable AUV named RAUVI was developed for underwater intervention, which was equipped with a robotic arm to operate the simple tasks [2]. With the advantage of autonomous manipulation, SAUVM can implement an

autonomous underwater intervention in the oceanic environment [3]. And an underwater recovery task including the target searching and returning the AUV back to the surface has been completed. Additionally, an underwater robot with six DOF (degrees of freedom) was equipped with an underwater vehicle-manipulator system for underwater intervention, which is a 3-DOF underwater manipulator [4], [5]. However, the underwater mechanical arms mounted on these AUVs are commonly enormous and the AUVs are commonly free floating vehicle platforms. As the weightlessness underwater, the underwater vehicle has to compensate for the movement caused by the movement of the mechanical arm and keep its position stable during the manipulation mission. Obviously, it needs a complex control system.

Consequently, a small-sized, highly maneuverable and deployable ROV began to be used as the manipulator. An agent vehicle was developed as a manipulator of a main AUV and is connected to it by a smart cable for underwater manipulations [6]. In our lab, we designed a microrobot as a grasper of a small-sized AUV to implement underwater tasks [7]. In addition, an ICPF actuator-based crayfish-inspired microrobot was designed and developed as a manipulator of a father-son robot system in our previous research [8]. In order to adapt to complex underwater environments and easily be sent out and recycled, an amphibious spherical robot was designed and developed for the father-son robot system [9]. The microrobot was connected to the amphibious father robot by several copper wires. However, the wires and cables will restrict the performance of manipulation of the underwater vehicles and cause the manipulators to be easily snagged by the aquatic plants and rocks.

Accordingly, an ICPF actuator-based wireless microrobot is proposed as the mechanical arm of the father-son robot system in this paper. The microrobot is actuated by nine ICPF actuators to implement the walking, rotating, floating, swimming and grasping motions. To realize the communication between the father robot and the son robot, we proposed a new cableless communication method, which is to use a blue LED-based underwater optical communication system. The father robot with a high mobile velocity uses two blue LEDs to control the motion of microrobots by sending signals, and uses a Wi-Fi camera module to catch the signals from the microrobots to realize the closed-loop control of the

communication protocol. In addition, two light sensors are mounted on the microrobot for receiving the instructions from the father robot. And two indicator lights are carried on the microrobot to indicate that the microrobot has received the signal successfully.

The remainder of this paper is organized as follows. We described the father-son robot configuration in section II. In section III, we introduced the design, motion mechanism and electrical system of the wireless microrobot. Then, a new communication protocol was proposed in section IV. In section V, the underwater experiments were conducted to evaluate the performance of the microrobot. And the communication experiments were carried out to verify the proposed communication protocol. Finally, we drew the conclusions in section VI.

II. FATHER-SON ROBOT CONFIGURATION

A. An Amphibious Spherical Father Robot

We propose a father-son robot system for the underwater intervention, which used the microrobots as the mechanical arms, as shown in Fig. 1. And an amphibious spherical father robot with two actuation modes, including the water-jet propulsion and quadruped walking modes, was developed in our previous research [9]. The amphibious robot has the advantages of walking from the ground to the water without the ship support, and vice versa [10], [11]. And the symmetry of the spherical shape provides the superiority of flexibility [12], [13], [18].

The amphibious spherical father robot consists of a sealed transparent upper hemispheroid, two transparent quarter spherical shells that can be opened, a plastic oblong plate for carrying the microrobots, and four actuating units, which are fastened to a plastic circular plate [14], [15]. The amphibious father robot can take the microrobots from the ground to the water without manpower in a high speed and can keep itself still for precise manipulation of the microrobots underwater.

The father-son robot system uses an AVR ATMEGA micro-controller to control each servo motor and water-jet propeller. A Wi-Fi camera module is utilized on the father robot to realize the closed-loop control to the communication protocol for catching the feedback signals from the microrobots. Two sets of blue LED lights are installed symmetrically along the central plane on the edge of the two openable quarter spherical shells, as shown in Fig. 1, which are used to send control signals to the microrobots.

Furthermore, for receiving the microrobots, another set of blue LED lights are installed on the plastic oblong plate of the father robot to send the receiving signals to the microrobots.

B. Microrobots

The microrobots carried on the father robot are driven by the ICPF actuators. To operate the underwater mission of the object recovery, the wireless microrobots should be capable of multi-functional motions, including being launched, finding and recycling the target object remotely controlled by the father robot and getting back to the plastic oblong plate of the father robot actively. Two light sensors are mounted on the

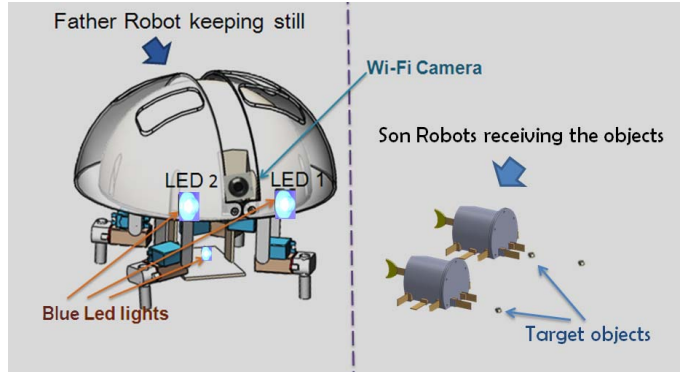


Fig. 1 Father-son robot configuration

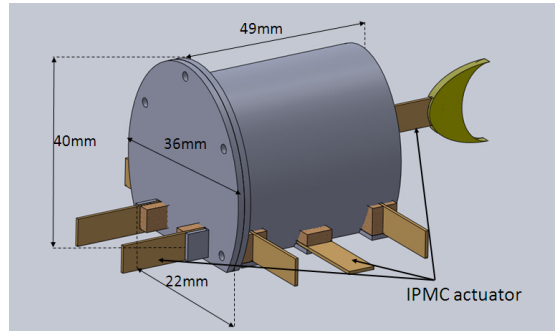


Fig. 2 The proposed wireless microrobot

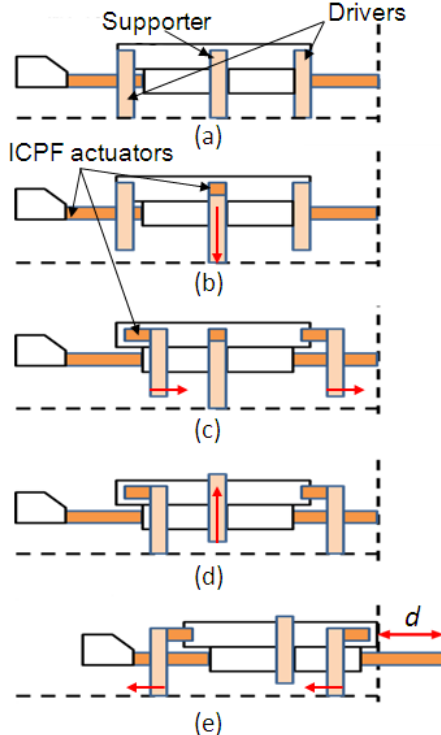


Fig. 3 One step cycle of walking motion: (a) In the initial state; (b) Two supporters bending downwards to lift the body up; (c) Four drivers bending forwards; (d) Two supporters bending upwards to use the drivers to lift the body up; (e) Four drivers bending backwards to make the robot move forwards. (The red arrows indicate the moving direction of each leg)

front part of each microrobot to receive the control signals from the father robot, which controls two sets of the blue LED lights to light up/off orderly. Additionally, a red LED light and a green LED light mounted on the microrobot are used as the indicator lights to show the indication signals of receiving the infrared signals. Without cables, the microrobot can be launched by one father robot to recycle object and then received by another one. Fig. 2 shows the conceptual design and the dimensions of the proposed microrobot.

III. DESIGN AND MOTION MECHANISM OF THE MICROROBOT

A. ICPF Actuator

ICPF is a novel material made of an ionic polymer membrane plated with gold electrodes chemically on both sides [17]. When we apply an electric stimulus to this material, ICPF will generate a bending deformation because of the change in the chemical structure. When the voltage is applied on both electrodes of ICPF, it will bend towards the positive electrode.

ICPF actuators have the advantages of soft characteristic, compact structure, low noise driving, low voltage driving, driving in water or wet environments, and having the similar density to the water. With the property of quick response, ICPF actuators can be used as the oscillating fins for swimming motion, and legs for walking motion.

B. Structure of the Underwater Microrobot

A biomimetic cableless microrobot is proposed to be the mechanical arm of the father robot, as shown in Fig. 2. The microrobot consists of a main body, a transparent front cover and nine ICPF actuators, including two fingers for grasping motion, one tail fin for swimming motion, and two supporters and four drivers for walking, rotating and floating motions. Nine actuators are all 20 mm long, 5 mm wide and 0.2 mm thick and have one degree of freedom. Two light sensors are mounted on the front part of the microrobot right behind the transparent cover. Moreover, two indicator lights are carried on the microrobot.

C. Mechanism of the Walking/Rotating Motion

The microrobot is actuated by four drivers and two supporters which are driven by the square signals with the same oscillating frequency. And the phase of the supporters are set to lag behind the phase of the drivers by 90°. Fig. 3 shows one step cycle of the moving forward motion of the microrobot. When the four drivers bend to the same direction, the robot will walk forwards or backwards. When the drivers on different side of the robot bend to two different directions, the robot will rotate in clockwise or counterclockwise.

We assumed that the tip displacement of ICPF actuator is equal to $d/2$. Then an average speed of the microrobot can be achieved by (1).

$$v = d * f \quad (1)$$

where d is the moving distance of the microrobot in one step cycle, v is the average speed and f is the control frequency.

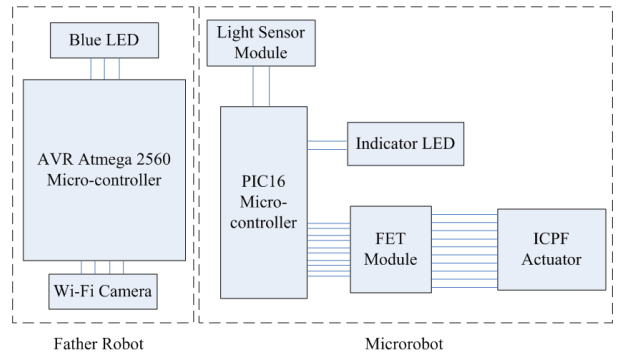


Fig. 4 Control system of the father-son robot system

D. Electrical System and Power Supply

The control center of the microrobot is shown in Fig. 4. It is based on a PIC16F1827 micro-controller, which is suitable for the microrobot due to the compact structure, and it uses three ADC (analog to digital conversion) channels to control two light sensors to receive the optical data from the father robot. Furthermore, ten input/output ports are used to drive the ICPF actuators and control the indicator lights, which will be lightened after the light sensor received the optical signals. The spherical father robot is controlled by an AVR Atmega2560 micro-controller. Three sets of blue LED lights are controlled by three input/output ports. Two sets of them are used to send eight blue LED signals in a different order (only one set of lights will be turned on in one time) to microrobot, which can drive the robot to realize different functions. The third one is utilized to receive the microrobots.

The microrobot uses the batteries to provide power to both the PIC micro-controller and the ICPF actuators.

IV. COMMUNICATION PROTOCOL

A new communication protocol is proposed to facilitate the communication between the amphibious father robot and the microrobots. To control the microrobot to complete the assigned work, an 8-bit binary encoding consisted of one parity bit, three control bits and four numerical bits need to be sent to the microrobot from the father robot. The parity bit indicates whether a correct 8-bit binary encoding is sent or not. Also, three control bits that can form eight different combinations are employed to correspond to eight different functions of the microrobot, as shown in Table I. Additionally, four numerical bits indicate the numerical values of the corresponding function of the microrobot.

For the microrobot, two light sensors (sensor 1 and sensor 2) attached to the front part are applied to receive binary bits from the father robot. Binary value 0 is defined when the difference of the received voltage between sensor 1 and sensor 2 is greater than 20 mV. On the contrast, binary value 1 is defined when the difference of the received voltage between sensor 1 and sensor 2 is less than -20 mV. The initial voltage value of the two light sensors is 0. The received voltage value of the light sensor will be changed as a function of the intensity of the blue LED light and the value increases smoothly as the distance between the sensor and the blue LED light decreases.

TABLE I. Binary encoding rules for the motion control of the microrobot

Parity bit	Control bits			Numerical bits				Functions	
	Bit7	Bit6	Bit5	Bit4	Bit3	Bit2	Bit1	Bit0	
1	0	0	0		$0 < N \leq 15$				Walking forward N steps
1	0	0	1		$0 < N \leq 15$				Walking backward N steps
1	0	1	0		$0 < N \leq 15$				Rotating in clockwise
1	0	1	1		$0 < N \leq 15$				Rotating in anticlockwise
1	1	0	0	0	0	0	0		Grasping
				0	0	0	1		Loosening
1	1	0	1		$0 < N \leq 15$				Floating N steps
1	1	1	0		$0 < N \leq 15$				Swimming N steps
1	1	1	1	0	0	0	0		Returning (Received by father robot)
				1	1	1	1		Stop all the motions
0	0~8			0~15					Error codes

The father robot sends a binary bit to the microrobot by two sets of blue LED lights located on the left side (Blue LED 1) or the right side (Blue LED 2) of the quarter spherical shell respectively, as shown in Fig. 1. When the father robot turns on the Blue LED 1, the voltage value received by sensor 1 is greater than that received by sensor 2 due to the relatively smaller distance between Blue LED 1 and sensor 1. Thus, the microrobot receives binary value 0. Inversely, the microrobot receives binary value 1 when the Blue LED 2 is turned on. The corresponding indicator light (red LED light or green LED light) will be lightened according to the received binary value 0 or 1 respectively, which provides a feedback to the father robot.

The control protocol between the father robot and the microrobot is described as following:

- 1) The microrobot turns on the red and green indicator lights simultaneously and keeps the two lights on for two seconds to send the father robot a status feedback that the microrobot is waiting for a binary value of an 8-bit control instruction;
- 2) The father robot detects the status of the red and green LED lights by the camera module. If the two LEDs are both lightened, the father robot starts to send an 8-bit control instruction;
- 3) The father robot sends an 8-bit control instruction made up of the binary value 0 and 1 by turning on the Blue LED 1 or Blue LED 2 respectively;
- 4) The microrobot receives the 8-bit control instruction by computing the difference of the received voltage between the two sensors and then turns on the red LED light or green LED light according to the received binary value 0 or 1 respectively;
- 5) The father robot detects the feedback from the microrobot through the camera module. If the microrobot receives a correct bit, the father robot prepares to send the next binary bit. Otherwise, father robot sends an error code with parity bit 0 to the microrobot to stop the current communication;
- 6) The process repeats from step 1) to step 5) until the microrobot receives a correct 8-bit control instruction; then the microrobot turns off the red and green LED lights

simultaneously and starts the corresponding work according to the 8-bit control instruction. After the work is completed, the two indicator lights will be lightened.

V. PROTOTYPE MICROROBOT AND EXPERIMENTS

For realizing the underwater operations in complicated environments, a father-son underwater robot system with a new cableless communication method is proposed. To complete the whole system, the basic motions of the microrobot and the communication method are verified.

A. Prototype Microrobot and Performance Evaluation of the ICPF Actuators

A prototype biomimetic wireless underwater microrobot is developed, as shown in Fig. 5(a). The power supply of the microrobot is two 3.7V Li batteries with a 200mAh capacity. The control center of the microrobot is based on a PIC16 microcontroller. The control circuit of the microrobot is shown in Fig. 5(b). The volume of the body of the microrobot is 62.314 cm^3 and the weight of it is 68.245 g.

Before we decide the value of the applied control voltage, we did the performance evaluation of the ICPF actuator. The tip displacement of the ICPF actuator is related to the applied voltage. In order to get an appropriate voltage for the ICPF actuator control, we apply different voltages on both electrodes of ICPF to measure the change of the tip displacement with time. We conduct the experiments in both water and salt water with a density of 3.4%. During the experiments, as the change of the tip displacement at a control voltage over 5V become large with time which is not suitable for the microrobot actuation, the control voltage is set in a range from 1V to 5V. Figs. 6 and 7 show the experimental results of the change of the tip displacement of the ICPF actuator with time in water and salt water respectively. From the results, applying a voltage over 4V to the ICPF actuator shows a better performance of tip displacement. Considering that a large tip displacement will be better for the movement of the robot, the driving voltage is set to be 5V.

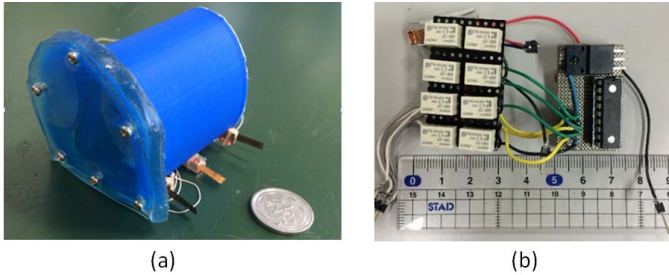


Fig. 5 (a) The prototype microrobot and (b) the control circuit

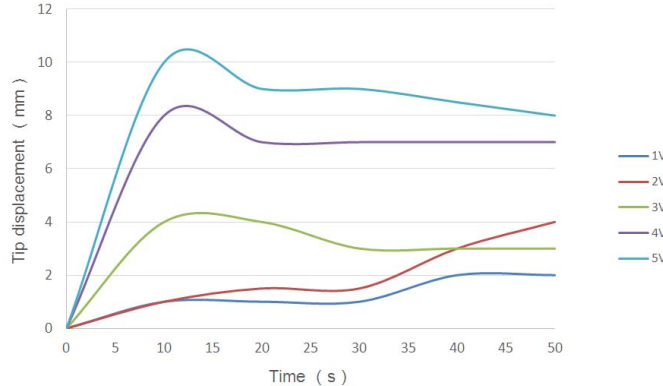


Fig. 6 Experimental results of the change of the tip displacement of the ICPF actuator with time (in water)

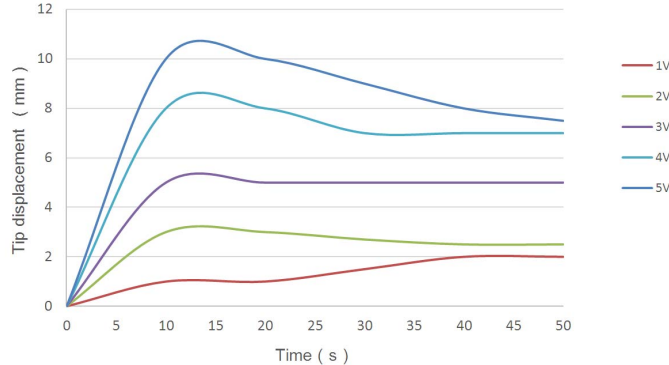


Fig. 7 Experimental results of the change of the tip displacement of the ICPF actuator with time (in salt water)

B. Experiments of Walking and Rotating Motions in a Water Tank

Walking and rotating experiments of the microrobot were conducted in a water tank to evaluate the performance of the robot at a given control voltage of 5V. During the experiments, we changed the control frequency and calculated the walking speed and rotational speed of the microrobot in each signal by recording the time separately. All experiments were repeated five times at a set of control signals to achieve an average speed. The experimental results of walking and rotating motions are shown in Figs. 8 and 9 respectively. From the results, a maximum walking speed of 9.85 mm/s and a maximum rotational speed of 13.13 %/s were achieved at a control frequency of 1.25 Hz. From the results of our previous [16], the tip displacement of the ICPF actuator will decrease as a function of control frequency. According to (1), the average

speed of the robot is related to the step distance and the frequency. Consequently, with the control frequency increasing, the speed will increase at first and then decrease to zero.

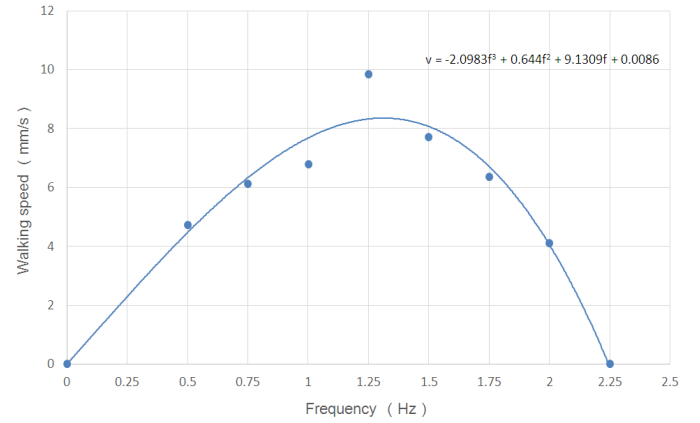


Fig. 8 Experimental results of the walking motion

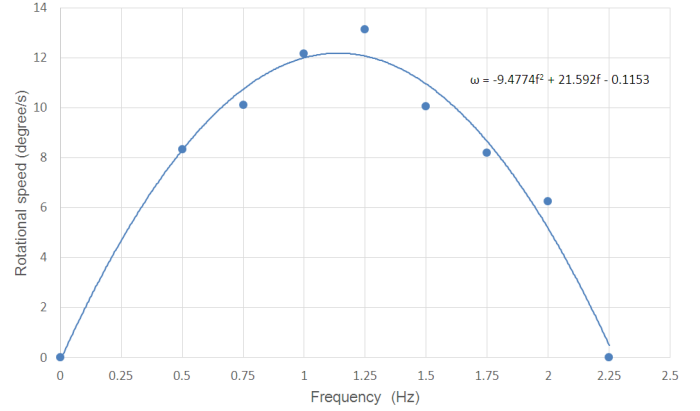


Fig. 9 Experimental results of the rotating motion

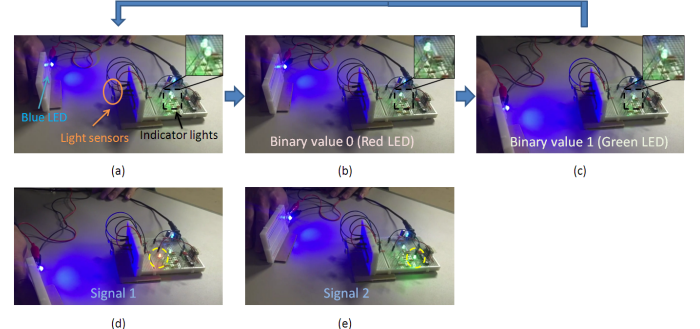


Fig. 10 Communication experiments: (a) The blue LED light can be lightened to send optical signals when the two indicator lights are on; (b) The indicator light on the left side is turned on when the light sensor on the left side receives a higher light intensity than the other side; (c) The indicator light on the right side is turned on when the light sensor on the right side receives a higher light intensity than the other side; (d) When the micro-controller receives signal 1, the red LED is lightened; (e) When the micro-controller receives signal 2, the green LED is lightened

C. Communication Experiments

Before installing the light sensors on the robot, the performance of the photodiode was evaluated in our previous research [8]. We conducted the underwater experiments of the optical communication system, in which a blue LED light and a photodiode are employed as the transmitter and receiver respectively. From the previous results, the photodiode can detect the blue LED at a maximum distance of 120 cm and the detectable angle is in a range from -60° to 60°. Within this range, the light sensor can detect the signal strength emitted by the blue light source well.

To realize the communication between the father robot and the microrobot without cables, a new communication protocol is proposed. Moreover, an experiment setup is established for the communication experiments to verify the proposed communication protocol, as shown in Fig. 10 (a). The experiment setup is consisted of an blue LED light, a PIC micro-controller of microrobot, two indicator lights, two LED lights, in which the red LED indicates a successful receiving of the signal 1 (a specified 8-bit binary encode) and the green LED indicates a successful receiving of the signal 2 (another specified 8-bit binary encode). Using this experiment setup, two kinds of experiments were conducted by sending two kinds of signals: signal 1 and signal 2, as shown in Fig. 10. During the experiments, the process repeats 8 times from step (a) to (c) until the microrobot receives an 8-bit control instruction. When the microrobot receives signal 1, the red indicator light is turned on, as shown in Fig. 10 (d); when it receives signal 2, the green light is turned on, as shown in Fig. 10 (e). From the results, we know that this communication protocol can be used to realize the communication between the father and son robots.

VI. CONCLUSIONS

In this paper, a biomimetic wireless microrobot has been developed as the mechanical arm of the father-son robot system. The microrobot is actuated by nine ICPF actuators. It can implement the walking, rotating and grasping motions. In order to realize the communication between the father robot and son robots, a new cableless communication method was proposed. The father robot is able to carry the ICPF actuator-based wireless microrobot and send the optical signals to control the motion of it. Two light sensors were equipped on the microrobot to receive the optical data from the father robot and two indicator lights were used for the closed-loop control to the communication protocol.

The walking and rotating experiments were conducted to evaluate the performance of the robot. From the experimental results, a maximum walking speed of 9.85 mm/s and rotational speed of 13.13 °/s were achieved at a control frequency of 1.25 Hz. Finally, the communication experiments were carried out to verify that the proposed communication protocol can be used for the communication between the father and son robots.

ACKNOWLEDGMENT

This research is partly supported by National Natural Science Foundation of China (61375094), Key Research Program of the Natural Science Foundation of Tianjin

(13JCZDJC26200), National High Tech. Research and Development Program of China (No.2015AA043202), and SPS KAKENHI Grant Number 15K2120.

REFERENCES

- [1] B. Jun, P. Lee, S. Kim, "Manipulability analysis of underwater robotic arms on ROV and application to task-oriented joint configuration", *Journal of Mechanical Science and Technology*, Vol. 22, pp. 887-894, 2008.
- [2] G. De Novi, C. Melchiorri, J. C. Garcia, P. J. Sanz, P. Ridao, G. Oliver, "A New Approach for a Reconfigurable Autonomous Underwater Vehicle for Intervention", *Systems Conference, 2009 3rd Annual IEEE*, pp. 23-26, 2009.
- [3] G. Marani, S. Choi, J. Yuh, "Underwater autonomous manipulation for intervention missions AUVs", *Ocean Engineering*, Vol. 36, pp. 15–23, 2009.
- [4] S. Mohan, J. Kim, "Indirect adaptive control of an autonomous underwater vehicle-manipulator system for underwater manipulation tasks", *Ocean Engineering*, Vol. 54, pp. 233–243, 2012.
- [5] S. Mohan, J. Kim, "Coordinated motion control in task space of an autonomous underwater vehicle-manipulator system", *Ocean Engineering*, Vol. 104, pp. 155–167, 2015.
- [6] S.-C. Yu, J. Yuh, J. Kim, "Armless underwater manipulation using a small deployable agent vehicle connected by a smart cable", *Ocean Engineering*, pp. 149-159, 2013.
- [7] C. Yue, S. Guo, L. Shi, "Design and Performance Evaluation of a Biomimetic Microrobot for the Father-son Underwater Intervention Robotic System", *Microsystem Technologies*, DOI: 10.1007/s00542-015-2457-z, 2015.
- [8] M. Li, S. Guo, J. Guo, H. Hirata, H. Ishihara, "Development of a Biomimetic Underwater Microrobot for a Father-son Robot System", *Microsystem Technologies*, DOI 10.1007/s00542-016-2817-3, 2016.
- [9] M. Li, S. Guo, H. Hirata, H. Ishihara, "Design and Performance Evaluation of an Amphibious Spherical Robot", *Robotics and Autonomous Systems*, doi:10.1016/j.robot.2014.11.007, Vol. 64, pp. 21–34, 2015.
- [10] S. Zhang, X. Liang, L. Xu, M. Xu, "Initial Development of a Novel Amphibious Robot with Transformable Fin-Leg Composite Propulsion Mechanisms", *Journal of Bionic Engineering*, Vol. 10, No. 4, pp. 434-445, 2013.
- [11] G. Dudek, P. Giguere, C. Prahacs, S. Saunderson, J. Sattar, L. Torres-Mendez, M. Jenkin, A. German, A. Hogue, A. Ripsman, J. Zacher, E. Milios, H. Liu, and P. Zhang, M. Buehler, C. Georgiades, "AQUA: An Amphibious Autonomous Robot", *Computer*, Vol. 40, No. 1, pp. 46-53, 2007.
- [12] X. Lin, S. Guo, K. Tanaka, and S. Hata, "Development and Evaluation of a Vectored Water-jet-based Spherical Underwater Vehicle", *INFORMATION: An International Interdisciplinary Journal*, Vol. 13, No. 6, pp. 1985-1998, 2010.
- [13] R. Chase, A. Pandya, "A Review of Active Mechanical Driving Principles of Spherical Robots", *Robotics*, pp. 1 – 21, 2012.
- [14] S. Guo, M. Li, C. Yue, "Performance Evaluation on Land of an Amphibious Spherical Mother Robot in Different Terrains", *Proceedings of 2013 IEEE International Conference on Mechatronics and Automation*, pp. 1173-1178, 2013.
- [15] S. Guo, M. Li, C. Yue, "Underwater Performance Evaluation of an Amphibious Spherical Mother Robot ", *Proceedings of 2013 IEEE International Conference on Information and Automation*, pp.1038-1043, Yinchuan, China, August 26-28, 2013.
- [16] S. Guo, M. Li, L. Shi and S. Mao, "A Smart Actuator-based Underwater Microrobot with Two Motion Attitudes", *Proceedings of 2012 IEEE International Conference on Mechatronics and Automation*, pp.1675-1680, 2012.
- [17] S. Kim, I. Lee and Y. Kim, "Performance enhancement of IPMC actuator by plasma surface treatment", *Journal of Smart Material and Structures*, Vol. 16, pp.N6-N11, 2007.
- [18] Y. Li, S. Guo, C. Yue, "Preliminary Concept of a Novel Spherical Underwater Robot", *International Journal of Mechatronics and Automation*, Vol.5, No.1, pp. 11-21, 2015.